International Journal of Biological Macromolecules 186 (2021) 849–863

Contents lists available at ScienceDirect

International Journal of Biological Macromolecules

journal homepage: www.elsevier.com/locate/ijbiomac

Blockade of CD73 using siRNA loaded chitosan lactate nanoparticles functionalized with TAT-hyaluronate enhances doxorubicin mediated cytotoxicity in cancer cells both *in vitro* and *in vivo*

Armin Mahmoud Salehi Khesht [a,b,1], Vahid Karpisheh [a,c,1], Parisa Sahami Gilan [d], Lyubov A. Melnikova [e], Angelina Olegovna Zekiy [f], Mahdis Mohammadi [g], Mohammad Hojjat-Farsangi [h], Naime Majidi Zolbanin [i,j], Ata Mahmoodpoor [k], Hadi Hassannia [l], Leili Aghebati-Maleki [a], Reza Jafari [m,*], Farhad Jadidi-Niaragh [a,n,**]

[a] *Immunology Research Center, Tabriz University of Medical Sciences, Tabriz, Iran*
[b] *Department of Biochemistry, Faculty of Materials Engineering, Islamic Azad University, Najafabad Branch, Najafabad, Iran*
[c] *Student Research Committee, Tabriz University of Medical Sciences, Tabriz, Iran*
[d] *Medical Biology Research Center, Health Technologies Institute, Kermanshah University of Medical Sciences, Kermanshah, Iran*
[e] *Finance University under the Government of the Russian Federation, Moscow, Russian Federation*
[f] *Department of Prosthetic Dentistry, Sechenov First Moscow State Medical University, Moscow, Russia*
[g] *Department of Biology, Faculty of Sciences, Golestan University, Gorgan, Iran*
[h] *Bioclinicum, Department of Oncology-Pathology, Karolinska Institute, Stockholm, Sweden*
[i] *Department of Pharmacology and Toxicology, Faculty of Pharmacy, Urmia University of Medical Sciences, Urmia, Iran*
[j] *Experimental and Applied Pharmaceutical Sciences Research Center, Urmia University of Medical Sciences, Urmia, Iran*
[k] *Department of Anesthesiology, School of Medicine, Imam Reza Medical Research & Training Hospital, Tabriz University of Medical Sciences, Tabriz, Iran*
[l] *Immunogenetic Research Center, Mazandaran University of Medical Sciences, Sari, Iran*
[m] *Solid Tumor Research Center, Cellular and Medicine Research Institute, Urmia University of Medical Sciences, Urmia, Iran*
[n] *Department of Immunology, Faculty of Medicine, Tabriz University of Medical Sciences, Tabriz, Iran*

ARTICLE INFO

Keywords:
Cancer
CD73
Doxorubicin
Nanoparicle
siRNA

ABSTRACT

Chemotherapy drugs are still one of the first treatment options used in many cancers; however, problems such as cytotoxic side effects on normal cells after systemic administration and resistance to treatment have reduced the use of chemotherapeutics day by day. Targeted delivery of these drugs to the tumor site and sensitization of cancer cells to death induced by chemotherapy drugs are ways that can overcome the limitations of the use of these drugs. In this study, we designed and generated a novel nanocarrier composed of chitosan lactate nanoparticles (NPs) functionalized by HIV-1 derived TAT peptide (Transactivating transcriptional activator) and hyaluronate (HA) to deliver CD73 siRNA and doxorubicin to 4T1 and CT26 cancer cells, both *in vivo* and *in vitro*, as a novel combinatorial treatment strategy. The CD73 molecule plays a key role in many cancer cell behaviors such as proliferation, angiogenesis, metastasis, imunosuppression, and resistance to chemotherapy. Therefore, we decided to reduce the side effects of DOX by simultaneously transmitting CD73 siRNA and DOX by CL-TAT-HA NPs, increase the susceptibility of cancer cells to DOX-induced cell death, and stimulate anti-tumor immune responses, for the first time. These results indicated that simultaneous transfer of CD73 siRNA and DOX to cancer cells (4 T1 and CT26) increased cell death and inhibited the prolifration and spread of cancer cells. Also, the preferential aggregation of NPs in the tumor microenvironment reduced tumor growh, promoted the survival of tumor-bearing mice, and induced anti-tumor immune responses. These findings indicate that CL-TAT-HA NPs are a good candidate for targeted siRNA/drug delivery to cancer cells and the simultaneous transfer of CD73 siRNA and DOX to cancer cells using this nanocarrier can be used to treat cancer.

* Corresponding author.
** Correspondence to: F. Jadidi-Niaragh, The Immunology Research Center, Tabriz University of Medical Sciences, Tabriz, Iran.
E-mail addresses: jafari.reza@umsu.ac.ir (R. Jafari), jadidif@tbzmed.ac.ir (F. Jadidi-Niaragh).
[1] These authors equally contributed in this study.

https://doi.org/10.1016/j.ijbiomac.2021.07.034
Received 31 January 2021; Received in revised form 10 April 2021; Accepted 4 July 2021
Available online 7 July 2021
0141-8130/© 2021 Published by Elsevier B.V.

1. Introduction

The tumor microenvironment, which is composed of cancer cells, stromal cells, various cytokines, and immune cells can suppress the immune responses, enhance progression and spread of carcinogenesis, and manage the response of the tumor cells to various types of treatment strategies [1,2]. Therefore, controlling and regulating the tumor microenvironment can prevent cancer progression in the body [3,4]. Our previous studies have shown that targeting cancer cells in the tumor microenvironment can be an ideal strategy for suppressing development and proliferation of tumor cells [5–8]. CD73 is one of the critical cell surface enzymes highly expressed in the tumor microenvironment by tumor and immunosuppressive cells [9]. CD73, which converts AMP to adenosine, is regulated by a variety of mechanisms and factors. Various studies have shown that CD73 is an essential molecule in the growth and proliferation, angiogenesis, invasion, spread of cancer cells, and drug resistance and its expression is increased in different types of cancer [10]. Thus, CD73 has become a useful therapeutic target with its function in cancer development, and various *in vitro* and *in vivo* researches have shown that targeted blockade of CD73 can be an effective treatment method for treating cancer patients [11].

Researchers have designed and used various approaches to inhibit target genes in the treatment of various diseases such as cancer. Among these methods, siRNA technique has been considered by researchers as an ideal treatment method due to its high ability to block target genes [12]. The simultaneous delivery of siRNA and chemotherapy drugs by nanoparticles (NPs) has become an effective cancer treatment strategy due to reducing drug side effects, increasing siRNA effectiveness, and synergistic effects. For example, the use of polymer NPs for the simultaneous delivery of chemotherapeutic drugs such as paclitaxel, doxorubicin (DOX) and siRNA can reduce the side effects of drugs and restore their sensitivity to chemotherapy and increase the drug accumulation in cancer cells [13]. Due to instability and low cell uptake *in vivo* and *in vitro*, siRNA requires a suitable carrier for transferring to tumor cells [14]. In the present study, we used DOX and anti-CD73 siRNA loaded in chitosan lactate (CL) NPs functionalized with TAT peptide and hyaluronate (HA) to deliver DOX and CD73 siRNAs to tumor cells. Chitosan is composed of chitin acetylation and contains *N*-acetyl-d-glucosamine (acetylated unit) and α-(1–4)-linked d-glucosamine (deacetylated units). It has been reported that chitosan derivatives can be produced by varying degrees of chitin acetylation [15]. Chitosan polymer, due to its unique features such as biodegradability, biocompatibility, and non-immunogenicity, can be used as a practical and ideal carrier in gene transfer and drug delivery systems [16]. Due to its positive charge, chitosan can bind to oligonucleotides (negatively charged) and protect them from destruction in effective delivery systems to tumor tissue [17]. Various studies have reported that various factors such as N/P (Nitrogen/Phosphorus) ratio, degree of acetylation, molecular weight [18], pH change, and chain length can regulate the cellular uptake of chitosan-based NPs loaded with oligonucleotides [19]. Previous *in vitro* investigations have reported that chitosan salts such as CL are suitable transfer nanocarrier for siRNA delivery [18,20]. In this study, we coated the CL NPs with HIV-1-derrived TAT peptide and HA to produce an appropriate delivery system. There are several methods to increase the efficiency and cell uptake of NPs into cancer cells. Conjugation of NPs with cell-penetrating peptides (CPPs) such as HIV-1 TAT is one method that can dramatically enhance the cell transfection rate. HIV-1 TAT CPP has a positively charged region that can bind to cell DNA [21]. HIV-1 TAT is rich in hydrophilic arginine and can transport proteins, peptides, plasmid DNA, and oligonucleotides to mammalian cells [22]. Also, the coating of nanocarriers with HA polymer due to HA interaction with CD44 molecule overexpressed in cancer cells can significantly increase NP uptake by cancer cells [23]. It has also been reported that HA may be suitable for gene and drug delivery methods due to its unique characteristics such as biodegradation and biocompatibility [24].

Although similar NPs such as CL [18], Ch-HIV-1 TAT [25], Ch-DOX [26], CL-PEG [27], Ch-PEG-PLGA [28], or CL-FA–PEG [29] have been used in previous studies, a novel CL-TAT-HA NPs developed in this study have advantages over them. For example, compared to the mentioned NPs, this generated nanoformulation is coated with HIV-1 TAT and HA that exhibits high cell transfection rate and high CD44-targeting potential. Our recent studies also confirmed the advantage of using HIV-1 TAT or HA for selective cancer cell targeting [30,31]. Both studies showed that targeting CD44 molecule expressed on cancer cells by HA-conjugated NPs is an efficient siRNA-delivery strategy. Based on a previous report that showed DOX could increase the expression of molecules involved in adenosine metabolism, including CD73 and CD39 in human breast cancer, melanoma, and leukemia cell lines [32], we decided to use a novel strategy to reduce an effective dose of DOX and inhibit the suppression of anti-tumor immune responses (due to upregulation of CD73 by DOX) *via* inhibiting the CD73 molecule. Therefore, our goal in this study was to use a novel nanocarrier system to facilitate the delivery of DOX to cancer cells, increase the effectiveness of the drug, reduce the effective dose of DOX, and prevent DOX-mediated CD73 upregulation. We also aimed to increase the susceptibility of cancer cells to DOX by inhibiting the expression of CD73 molecules and at the same time inducing anti-tumor immune responses.

This study proposed a new treatment method based on CD73 suppression and DOX delivery using CL-TAT-HA NPs in 4T1 and CT26 tumor cell lines. CL-TAT-HA NPs, which were synthesized for the first time, could deliver DOX and anti-CD73 siRNA to cancer cell lines and significantly suppressed the angiogenesis, invasion, proliferation, and migration of cancer cells.

2. Materials and methods

2.1. Reagents

Chitosan (MW: 50 kDa, DD: 96%) and hyaluronan were purchased from Cayman Chemical (Michigan, USA). EDC [1-Ethyl-3-(3-dimethyl aminopropyl) carbodiimide], sodium iodide [33], Sodium azide (NaN3) were obtained from Sigma-Aldrich (Mannheim, Germany). The synthetic TAT peptide (C (Npys) GRKKRRQRRR, purity: 92%) was obtained from Merck (Darmstadt, Germany). The MTT assay kit was bought from Santa Cruz (Santa Cruz, CA, USA). CD73 specific siRNAs and control siRNA were purchased from Sigma-Aldrich (Mannheim, Germany). Doxorubicin hydrochloride (DOX·HCl) was bought from Cayman Chemical (Michigan, USA).

2.2. Cell lines and mice

CT26 (colorectal) and 4T1 (breast cancer) murine cell lines were bought from the Pasteur Institute (Tehran, Iran). The cells were seeded in RPMI-1640 medium (ATCC, USA) with FBS (10%) and 100 units/ml antibiotics (Penicillin/streptomycin) (Sigma) and maintained at 37 °C in the CO_2 incubator (5%). BALB/c mice (8 weeks old) were obtained from Pasteur Institute (Tehran, Iran) and maintained under standard conditions. All animal tests were performed based on the instructions of Tabriz University of Medical Sciences' ethics committee. According to previous research [11,34], tumor bulk formed subcutaneously on the mouse's right flanks after injection of tumor cells (7×10^5), and the tumor bulk was measured every 48 h.

2.3. Generation and characterization of the CL-TAT-HA NPs loaded with siRNA/DOX

CL was produced according to the instructions of our previous research [35]. Briefly, 250 mg of chitosan powder (50 kDa) was added to 3 ml of the lactic acid solution and mixed for 25 min. In the next step, 20 ml of distilled water was added and mixed for 24 h. The synthesized CL was then collected and lyophilized. In the next step, the obtained mixture in distilled water was dialyzed for four days, and after

centrifugation, the supernatant was dried and frozen. Subsequently, mixture of CL (1 mg/ml in PBS, pH 7) was mixed with DOX solution (0.2 mg/ml in PBS, pH 8) and TPP (sodium tripolyphosphate) (0.5 ml, 0.6 mg/ml) at ambient condition for 24 h. The free DOX was removed from the CL-DOX solution through ultrafiltration by using a 1.0-K molecular weight cutoff membrane. To conjugate CL-DOX with TAT-HA, the TAT peptide (1.0 mg/0.3 ml PBS) was added and incubated at room temperature for 2 h and then kept at 4 °C overnight. Finally, 1 ml of HA (1 mg/ml) was added to the mixture, vortexed at 4000 rpm, and then incubated for one day. Eventually, 5 μg of siRNA solution was mixed with the CL-TAT-HA-DOX solution for 40 min and kept at room temperature for 1 h.

2.4. Measurement of size and zeta potential

The medium size, PDI (polydispersity indexes), and zeta potential of CL-TAT-HA NPs loaded with DOX/siRNA were evaluated by a dynamic light scattering device (Nano-ZS; MalvernInstruments, Malvern, UK). After dissolving in distilled water, the samples were measured at a detection angle of 95°, a wavelength of 640 nm, and a temperature of 26 °C.

2.5. Evaluation of NPs structure

Raman spectroscopy was used to evaluate the chemical bonds of CL and TAT peptide. The LabRAM HR spectrometer (CRAIC Technologies, Inc., USA) was also applied to analyze Raman spectra. The Raman spectrometer uses 16 mW power irradiation and a laser with a wavelength of 780 nm. Also, we applied the FTIR test to examine the chemical structure of synthesized NPs.

2.6. Scanning electron microscopy

SEM electron microscopy (Metropolitan-Vickers-UK) was performed to assess the morphology of NPs. Briefly, a drop of the nanoparticle mixture was placed on the lam and then dried in an incubator and covered with a layer of carbon in argon atmosphere. Finally, the samples were evaluated by Anix Emica software.

2.7. Stability of produced NPs in serum

Gel electrophoresis was used to assess the serum stability of CL-TAT-HA NPs loaded with siRNA/DOX, as described previously [36]. First, about 200 μl of siRNA-loaded CL-TAT-HA nanoparticles was added to 100 μl of FBS and stirred at room temperature. In the next step, the samples were analyzed by gel electrophoresis at 2, 4, 8, 16, 24, 36, and 48 h after incubation.

2.8. siRNA/DOX release profile assay

Based on our previous reports [37], the siRNA and DOX release patterns were evaluated. Briefly, CL-TAT-HA NPs loaded with siRNA and DOX were mixed in 5 ml of PBS (pH 6 and 7.4) and then moved to a dialysis membrane bag (8 kDa; SLS, UK). The dialysis bag was floated in 45 ml PBS under vibration (100 rpm) at room temperature. Finally, to evaluate the release profile, 1 ml of PBS at predetermined times (0, 2, 4, 8, 16, 24, 36, 48, 72 h) were collected and analyzed at 490 nm by UV spectrophotometer [38].

2.9. Cellular uptake assay

Flow cytometry technique (Becton-Dickenson, USA) and confocal microscope (Zeiss, LSM 880, Germany) were used to analyze the cellular uptake of NPs. In brief, 1×10^5 cells were cultured in six-well plates in 3 ml of RPMI medium with 10% FBS for 24 h. Then, the seeded cells were treated with CL-TAT-HA NPs loaded with FITC-siRNA and DOX and incubated for 48 h at 37 °C. These cells after washing with PBS (pH 7.4) were fixed with fixation buffer (5% formaldehyde + PBS) for 30 min. The cells were also stained with DAPI for 5 min to stain the cells' nucleus and then washed thoroughly with PBS. For flow cytometric testing, cells were seeded in a six-well plate and incubated until 70% confluence, transfected with NPs functionalized with TAT-HA or free NPs. The cultured cells were first washed with PBS and then separated from the plate bottom by trypsin. These cells were centrifuged four times and then washed again by PBS, and efficacy of transfection of NPs was analyzed by flow cytometry.

2.10. RNA extraction and qPCR

The qPCR assay was performed to investigate the mRNA expression of target genes after treatment with siRNA/DOX-loaded NPs in the CT26 and 4T1 cell lines. TonkBio™ RT reagent kit (Tonk Bioscience LLC., USA) was applied to obtain the total RNA, and cDNA synthesis kit (Sigma-Aldrich, USA) was applied to produce 450 ng cDNA of total RNA. The qPCR amplification reaction was applied by using StepOne Real-Time PCR System (Applied Biosystems Inc., USA) by applicating PCR Master Mix (SYBR Green, Thermo Scientific). Formula $2^{-\Delta\Delta CT}$ was applied to examine the target genes' quantitative mRNA expression level, and the melt curve was applied to analyze the target gene expression curve.

2.11. Western blot assay

Western blot test was applied to investigate the protein expression levels of CD73, Bcl-2, BIM, MMP2, and MMP9 factors. First, CT26 and 4T1 cells were treated with different treatment groups. The protein samples were then denatured and loaded by SDS buffer (Sigma-Aldrich, Mannheim, Germany) in 15% polyacrylamide gel and then moved to polyvinylidene difluoride membrane. In the next step, the polyvinylidene difluoride membrane was blocked at 37 °C for 2 h by TBS buffer (55 mM Tris, 0.2% T tween 20,155 mM sodium chloride, pH 7.4), and then incubated with primary anti-CD73 antibodies and anti-GAPDH mAbs (eBiosciences) at 6 °C for one day. Finally, after washing with PBST and adding HRP conjugated Abs (LifeSpan BioSciences) the membrane was incubated for 2 h. Western blot detection kit (Cayman Chemical, Michigan, USA) was performed to analyze the reaction bands.

2.12. Assessment of Doxorubicin IC50

To investigate IC50 of free DOX and DOX-loaded NPs, CT26 and 4T1 cells were treated with accumulating concentrations of DOX in the 96-well plates and incubated for 24 h. IC50 of free DOX and DOX-loaded NPs assessed using an ELISA Reader at 570–630 nm (Organon Teknika, Turnhout, Belgium).

2.13. Investigation of siRNA loading efficiency

By measuring the concentration of unloaded siRNA in the supernatant of centrifuged CL-TAT-HA NPs, the loading efficiency of siRNA in CL-TAT-HA NPs was investigated. In summary, 250 μl of NP-CL-TAT-HA (1 mg/ml) were loaded with siRNA (2, 4, 8, 10, and 20 μg) and centrifuged at 16,000 rpm for 15 min and the siRNA content in the supernatant was then assessed by microplate reader. Finally, the loading efficiency of siRNA was obtained applying the following equation [6]:

$$\text{Loading efficiency } (\%) : [1 - (\text{OD of siRNA in the supernatant}/\text{OD of primary siRNA amount})]\ 100$$

2.14. Examination of drug encapsulation and drug loading efficiency

To assess the DOX loading and encapsulation efficiency, 6 mg of the CL-TAT-HA NPs was added in 12 ml of phosphate buffer (0.1 mg/ml). Then the increasing doses of DOX (1 μM) (5, 6, 7, 8, 9, 10, 11, 12, 13, 14 and 15 μl) were dissolved in the solution and after 2 h, the solution was centrifuged (20 min, 16,000 rpm) and the amount of unencapsulated DOX was measured by using a UV spectrophotometer at 350 nm. DOX loading and encapsulation efficiencies were obtained by the following equations [39]:

$$\text{Loading capacity}\ (\%) : (\text{Total amount of drug} - \text{nonencapsulated drug}/\text{weight of NPs})\ 100$$

$$\text{Encapsulation efficiency}\ (\%) : (\text{Total amount of drug} - \text{nonencapsulated drug}/\text{total amount of drug})\ 100$$

2.15. MTT toxicity assay

MTT assay was applied to examine the toxicity of CL-TAT-HA NPs loaded with siRNA and DOX in 4T1 and CT26 cell lines. In brief, 1.5×10^4 cancer cells were cultured in 96-well plates and after adherence to the plate treated with NPs loaded with optimized amounts of CD73-siRNA (70 pm siRNA) and DOX (100 nM for 4T1 and 300 nM for CT26). It should be noted that these concentrations of siRNA and DOX were used for all subsequent *in vitro* assays. After 24 and 48 h, the supernatant was removed, and fresh RPMI was replaced, then 20 μl of the MTT mixture was added to each well and incubated for 5 h. In the last step, after removing the supernatant, 150 μl/L of DMSO was added and incubated for 45 min. The toxicity of NP was assessed using an ELISA Reader at 600–640 nm (Organon Teknika, Turnhout, Belgium).

2.16. Investigation of cell apoptosis

Apoptotic effect of siRNA/DOX loaded NPs in CT26 and 4 T1 cells was evaluated by the Annexin V-FITC/PI apoptosis kit [31]. In brief, the 1×10^4 cells were cultured in six-well plates for 24 h. The cells were then treated with NP, free DOX, NP-DOX, NP-siRNA, and NP-siRNA-DOX treatment groups. After 24 h, the cells were centrifuged and washed 4 times with PBS and dissolved in 150 μl of annexin V binding buffer. Then, the cells were stained with 4 μl of annexin V-FITC at 37 °C for 30 min. Finally, 10 μl of propidium iodide was added to each tube 10 min before loading in devise. Finally, the results were detected and analyzed by flow cytometry assay.

2.17. BrdU assay

The BrdU assay was used to investigate the suppressive effect of siRNA/DOX-loaded CL-TAT-HA NPs on cancer cell proliferation [40]. Briefly, 4×10^3 CT26 and 4T1 cells were seeded in 96-well plates and incubated for 24 h. After treatment of cancer cells with siRNA/DOX loaded NPs for 24 h, 10 μl of BrdU solution was added to each well for 5 h. Then 100 μl of HRP-conjugated mouse anti-BrdU antibody was added to each well. Then, after one wash, 100 μl of tetramethyl benzidine was added. Finally, after 1 h, H_2SO_4 solution was applied to stop the reaction, and then the adsorption was measured using an ELISA Plate Reader at 630 nm.

2.18. Boyden chamber assay

Boyden chamber assay was applied to examine cell migration [31]. In this method, 1×10^5 CT26 and 4T1 cells transfected with siRNA/DOX loaded NPs and cultivated in upper chamber of 24-well boyden chamber plates containing polycarbonate filters with a pore size of 7 μm for 24 h. Also, RPMI-1640 supplement with 10% FBS was added to the lower chamber. The accumulated cells in lower chamber were stained with 1% crystal violet after fixation in methanol and counted by Olympus BX51 Fluorescence Microscope (Olympus, Tokyo, Japan).

2.19. Invasion assay

Invasion assay applied to assess the invasion potential of cancer cells. Briefly, the matrigel matrix was used to cover the upper surfaces of the transwell membranes. 5×10^4 of the 4T1 and CT26 cells cultured inside the transwell membrane treated with siRNA-DOX loaded NPs and were given 48 h to invade the other membrane. Non-invasive cells were removed from the upper part of the transwell membrane and the cells at the bottom of the filter were stained with Diff-Quick (Santa Cruz, CA, USA) and analyzed under a microscope.

2.20. Biodistribution and pharmacokinetics study of NPs

For biodistribution studies, 2 mg/kg CL-TAT-HA-DOX/siRNA and free-DOX were injected intravenously into four groups of tumor-bearing mice. Also, the same amount of saline was administered to control mice. Blood samples were then collected at 4, 8, 16, and 24 h after injection. Finally, after 24 h, to examine the level of DOX in vital organs such as kidney, liver, spleen, brain, heart, lung, and tumor tissue, all mice were killed, and then the organs were extracted, weighed, and lyophilized. In the next step, for homogenization of tissue and blood samples, acidic isopropanol Mini-Bead beater-1 (Biospec, OK) was added and centrifuged, and then the samples were maintained at 4 °C. The supernatant of centrifuged samples was applied to assess the DOX content intensity at 470 nm/520 nm.

2.21. Flow cytometry

The frequency of $CD8^+$ $CD44^+$ T cells was examined by flow cytometry using isotype control mAbs, CD44-PE, and CD8-FITC mAbs (Biolegend, CA, USA). In summary, 10^5 cells were mixed in 60 μl of staining buffer and incubated with fluorochrome-labeled mAbs for 1 h at 4 °C. The cells were washed three times and assessed using a FLOWJO software and BD FACS caliber flow cytometer (Becton-Dickenson) [41].

2.22. ELISA

ELISA test was performed to measure cytokines secreted by T cells.

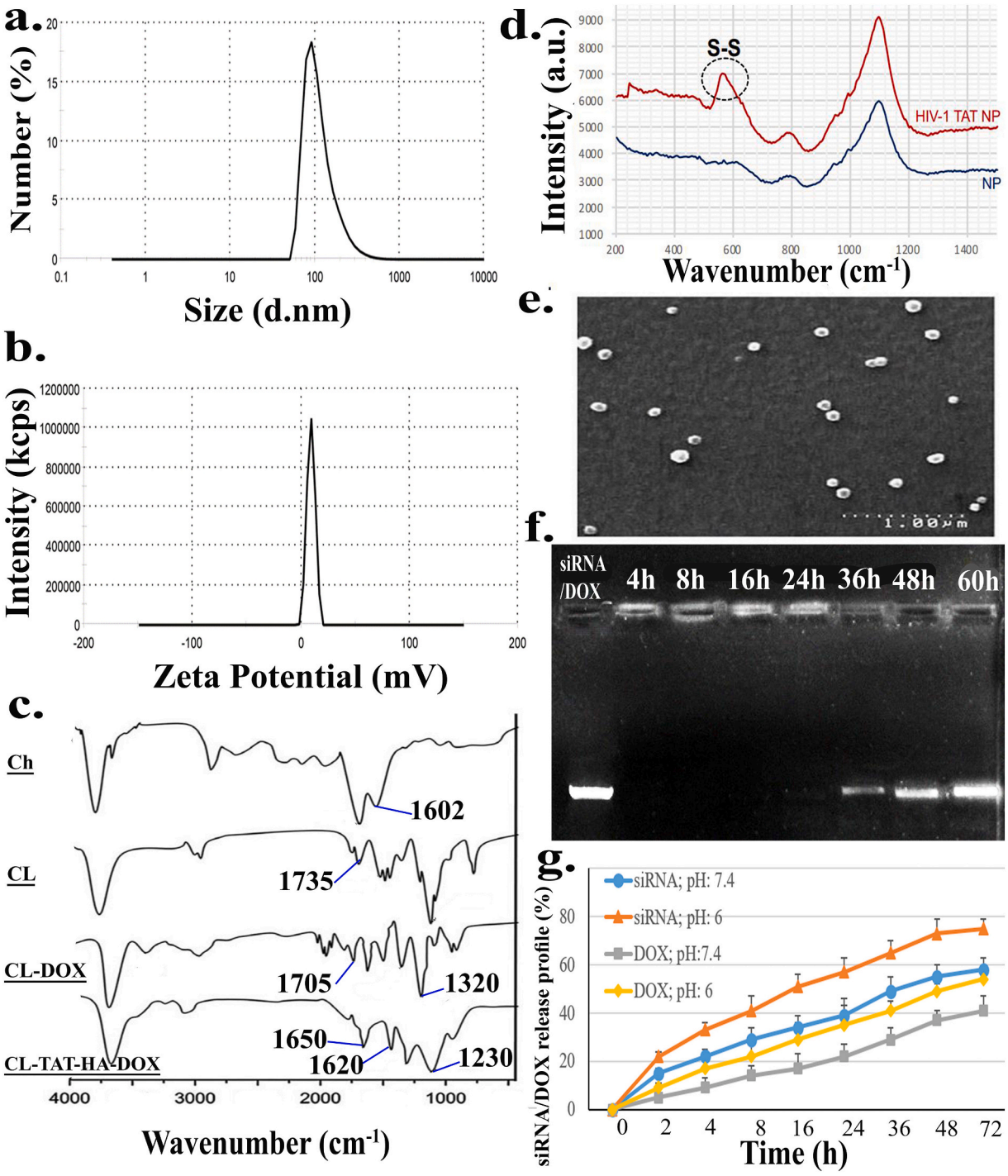

Fig. 1. Physicochemical properties of CL-TAT-HA NPs. NPs exhibited a size of 118 nm, PDI <0.24, and zeta potential of +9 mV (a and b). FTIR spectra demonstrate the bonds that indicate the formation of CL-TAT-HA NPs (c). Also, Raman spectroscopy was used to evaluate the chemical bonds of CL and TAT peptide reactions (d). NP's morphology was investigated *via* SEM (e). Gel electrophoresis was used to assess the serum stability of NPs loaded with siRNA and DOX (f). The siRNA/DOX release patterns of NPs were evaluated at 6 and 7.4 pH values (g). (CL: Chitosan lactate. TAT: Transactivating transcriptional activator. HA: Hyaloronate. NP: Nanoparticle. FTIR: Fourier-transform infrared spectroscopy. SEM: scanning electron microscope. DOX: Doxorubicin).

First, 10^5 T cells were stimulated with tumor cell lysate (TCL) (80 μg/ml) and then maintained in a culture medium at 37 °C and 5% CO_2. After three days, the supernatant was collected, and the secretion of IL-10, IL-4, IL-17, IFN-γ, and Granzyme B was evaluated based on the ELISA kits' instructions (Invitrogen, Carlsbad, USA) [27].

2.23. Histopathological analysis

In order to investigate the tumor histomorphometric characterization, dissected tumors were fixed in 10% buffered formalin and embedded in paraffin using standard methods. Three 4 μm serial sections were taken from each tissue and stained with hematoxylin and eosin (H&E). Then, sections were scanned using a digital slide scanner (Panoramic DESK, 3D Histech, Hungary).

Table 1
Primer sequences.

Gene name	Forward	Reverse
β-Actin	5′-GGTCATCACTATTGGCAACG-3′	5′-ACGGATGTCAACGTCACACT-3′
CD73	5′-TCCTGCAAGTGGGTGGAATC-3′	5′-TAGATGGGCACTCGACACTTG-3′
MMP9	5′-ACACGACATCTTCCAGTACC-3′	5′-CAGGAGGTCGTAGGTCACGTAGC-3
MMP2	5′-TGTGTCTTCCCCTTCACTTT-3′	5′-GATCTGAGCGATGCCATCAA-3′
BIM	5′-GAGATACGGATTGCACAGGA-3′	5′-ATTTGAGGGTGGTCTTCAGC-3′
BCL-2	5′-GGCTGGGGATGACTTCTCTC-3′	5′-ACAATCCTCCCCCAGTTCAC-3′

Table 2
The physicochemical characteristics of the generated nanoparticles.

Parameter	CL	CL-DOX	CL-TAT-HA-DOX	CL-TAT-HA-DOX/siRNA
Size	88 ± 3.2	96 ± 3.9	108 ± 4.1	118 ± 3.4
PDI	0.26 ± 0.04	0.29 ± 0.05	0.3 ± 0.06	0.24 ± 0.05
Zeta potential (mV)	12 ± 1.3	13.6 ± 1.7	11 ± 1.8	9 ± 1.6
siRNA encapsulation efficiency (%)				92
DOX encapsulation efficiency (%)		85		
DOX loading capacity (%)		8.4		

Evaluation of the microvessel density was performed based on the previous report [7]. Briefly, the sections were analyzed with two different magnifications (40× and 400×). In the first, the most vascular region of the tumor which is known as hot spot area was detected at 40× magnification. The number of microvessel was then evaluated in the hot spot region at 400× and stated as the number of microvessel/field. Moreover, the percentage of necrotic area in the tumor was examined by the Panoramic Viewer analysis software. In order to evaluate angiogenesis, the amount of tumor hemoglobin was examined by ELISA method as previously described [42].

2.24. Statistics

Statistical comparison of experimental outcomes was applied utilizing SPSS statistical software (SPSS, Chicago, IL, USA). The ONEWAY ANOVA method assessed the results. Kaplan-Meier method was also used for the estimation of the survival rate in the different therapeutic groups. *P* values less than 0.05 were considered significant. All tests were repeated twice and performed in triplicate.

3. Result

3.1. Physicochemical properties of chitosan lactate TAT-hyaluronate NPs

According to Fig. 1a, b and Table 1,the DLS results indicated that the CL-TAT-HA NPs loaded with siRNA/DOX have a size of 118 nm, PDI < 0.24, and zeta potential of +9 mV, which these results indicates that the CL-TAT-HA NPs had suitable properties for siRNA/DOX delivery.

As shown in Fig. 1c, the chemical structures of generated NPs was investigated by evaluating the FTIR spectra of chitosan, CL, CL-DOX, and CL-TAT-HA-DOX. Adsorption at 1602 cm^{-1} indicates the N—H group in chitosan, adsorption at 1735 cm^{-1} corresponds to the lactate-related carboxyl group (C=O) in CL, adsorption at 1320 cm-1 corresponds to C—C linkage of DOX and adsorption at 1650 cm^{-1} indicates the hyaluronate peak. Binding of HIV-1 TAT peptide to NPs is done by disulfide bonding. As shown in Fig. 1d, the Raman experiment results show that the TAT peptide is wholly bond to CL NPs' surface *via* the S—S bond at 510 cm^{-1}. SEM was applied to assess the morphology of NPs that exhibited a uniform spherical morphology (Fig. 1e).

The serum stability of siRNA/DOX-loaded CL-TAT-HA NPs was examined using gel electrophoresis at specified times. The results showed that siRNA release started at 24 h and NPs entirely emptied siRNA after 36 h (Fig. 1f). siRNA/DOX release profiles were examined in PBS at pH 7.4 (normal conditions) and pH 6 (tumor microenvironment conditions). As shown in Fig. 1g, the rate of siRNA/DOX release from CL-TAT-HA NPs increases with decreasing pH. The results also showed that in the first 24 h, NPs were able to start releasing their siRNA, and also, in the first 36 h, the NPs released 50% of their content.

Also, CL-TAT-HA and CL NPs' siRNA encapsulation efficiency was investigated using UV visible spectrophotometry at 480 nm. As shown in Table 2, the siRNA loading efficiency of CL-TAT-HA NPs was calculated to be 92%. In addition, DOX loading and encapsulation efficiencies of CL NPs were measured. According to the results, the DOX loading and encapsulation efficiencies were calculated to be 8.4% and 85%, respectively.

3.2. CL-TAT-HA NPs significantly entered cancer cells and suppressed the expression of CD73

The cellular uptake of functionalized NPs with TAT-HA and non-functionalized NPs was assessed by confocal microscopy. As shown in Fig. 2a, confocal microscopic results showed that NPs coated with TAT-HA had dramatically enhanced cellular uptake compared to non-targeted NPs. Besides, the cellular uptake of NPs was also examined by flow cytometry. The results showed that TAT-HA-conjugated NPs were transfected into about 78% of cancer cells, while free NPs were transfected into only 35% of cancer cells (Fig. 2b).

After confirming the entry of nanoparticles into cancer cells, their function in inhibiting CD73 gene expression was assessed by the qPCR and western blot tests. As demonstrated in Fig. 2c, The results showed that treatment of cancer cells with DOX increased CD73 expression (approximately 100%) while DOX translocation with NPs had less effect on increasing CD73 expression (approximately 40–60%). On the other hand, transfection of cancer cells with CD73 siRNA significantly suppressed the expression of this molecule (approximately 90%) and prevented the DOX-dependent CD73 upregulation (approximately 70%).

Also, the Western blot test was applied to examine the CD73 expression at the protein level. The results of the protein analysis were very similar to the results of assessing the mRNA level of the CD73 molecule (Fig. 2d).

3.3. Silencing of CD73 significantly enhanced DOX-induced cell cytotoxicity

The IC50 values of free DOX and DOX encapsulated by NPs in 4T1 (Fig. 3a) and CT26 (Fig. 3b) cell lines were examined by treatment of cancer cells with increasing concentrations of DOX for 24 h. The MTT test data showed that DOX encapsulation in NP has increased cytotoxicity, leading to a notable reduction in the IC50. As shown in Fig. 3c, the IC50 of DOX decreased from 1097 to 451 nM in CT26 cancer cells and from 437 to 138 nM in 4T1 cells.

Also, therapeutic groups' cytotoxicity, including untreated, free NPs, NP-CD73 siRNA, free DOX, NP-DOX, and NPs-CD73 siRNA-DOX on CT26 and 4T1 cancer cells after treatment with NPs loaded with CD73 siRNA (80 pM) and DOX (100 nM for 4T1 and 300 nM for CT26) was examined at 24 and 48 h. As shown in Fig. 3d–e, the data showed that although the CL-TAT-HA or CD73-siRNA loaded NP treatment groups alone do not have high toxicity to cancer cells, the combination therapy

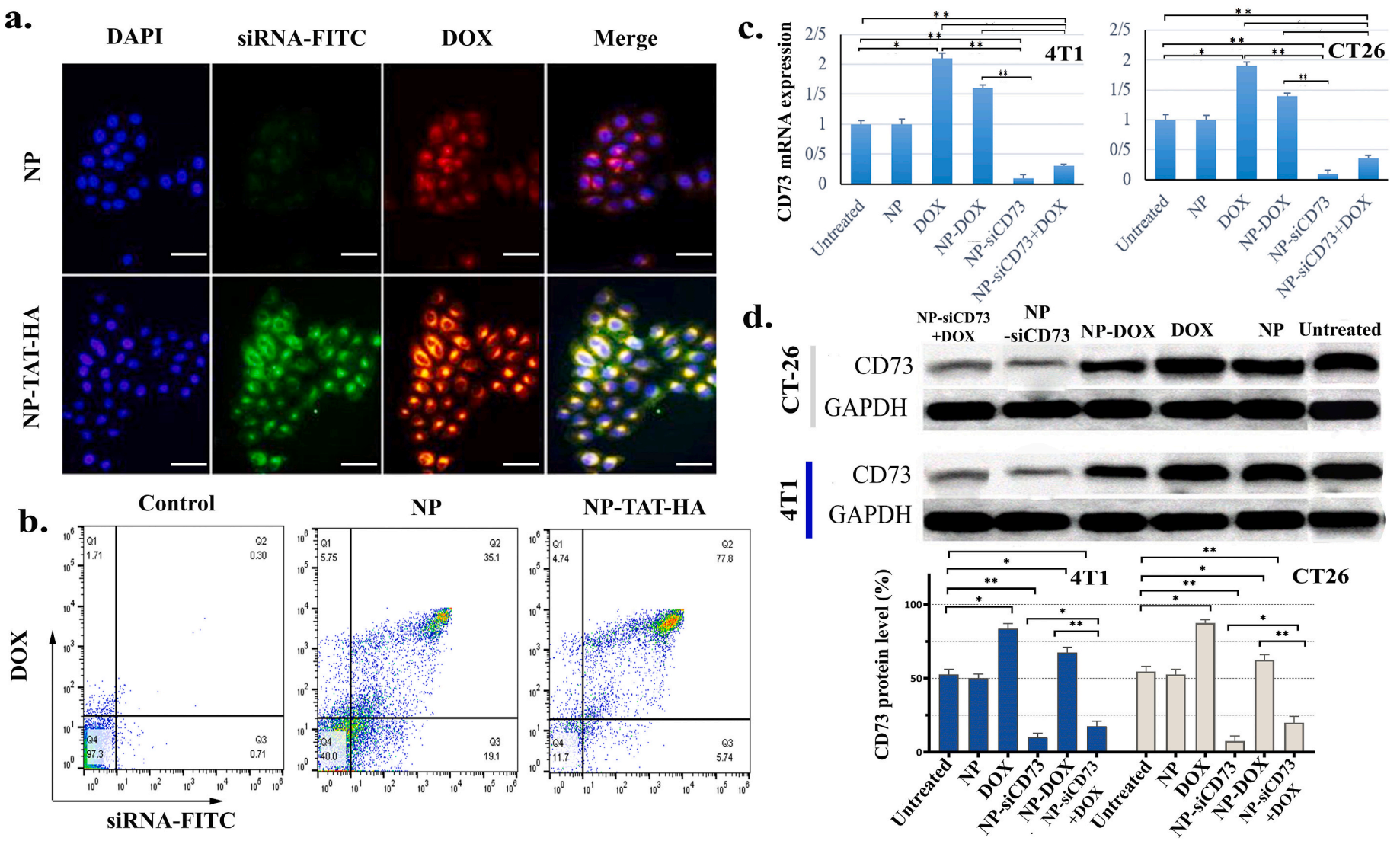

Fig. 2. CL-TAT-HA NPs are significantly uptaken by cancer cells and suppress the CD73 expression. Cellular uptake of TAT-HA-conjugated NPs and non-targeted NPs was examined by confocal microscopy (a) and flow cytometry (b) assays. The impact of siCD73 and DOX loaded CL-TAT-HA NPs on the CD73 expression in cancer cells was investigated by using qPCR (c) and western blot (d) assays. (qPCR: quantitative Polymerase Chain Reaction).

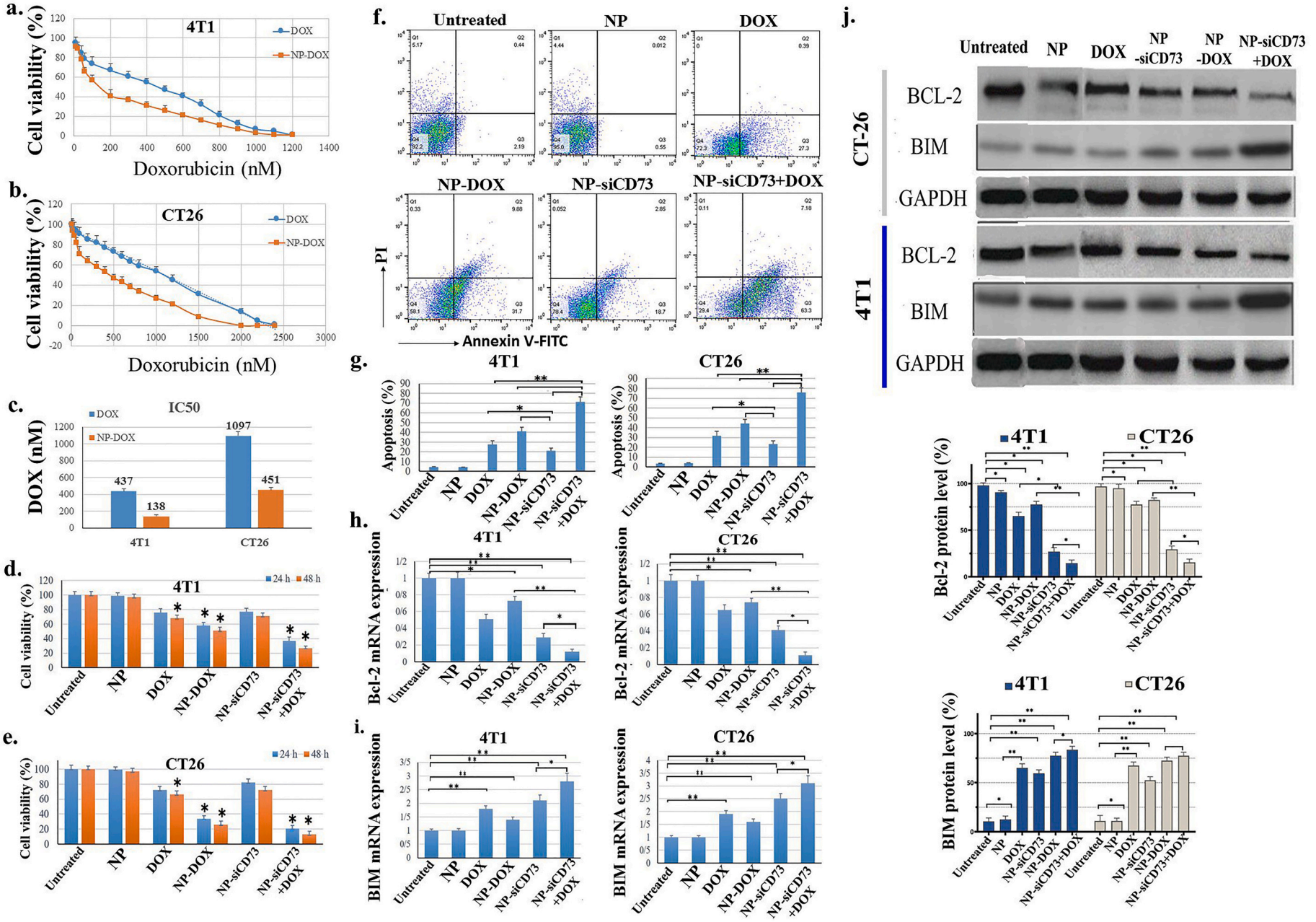

Fig. 3. Encapsulation of DOX by CL-TAT-HA NPs and silencing of CD73 significantly enhance DOX-induced cell cytotoxicity. The IC50 values of free DOX and DOX encapsulated by NPs in CT26 and 4T1 cell lines were evaluated by treatment of cancer cells with increasing amounts of DOX for 24 h (a–c). Bar charts demonstrate the cell viability of 4T1 and CT26 cell lines after treatment with NPs loaded with CD73 siRNA (80 pM) and DOX (100 nM for 4T1 and 300 nM for CT26) (d and e). Flow cytometry was performed to evalute treatment groups' apoptotic effects on cancer cells using the annexin V-FITC/PI staining (f and g). Cytotoxicity of siCD73/DOX loaded NPs was associated with the downregulation of Bcl-2 and the upregulation of BIM as evaluated by the qPCR and western blot assays (h–j).

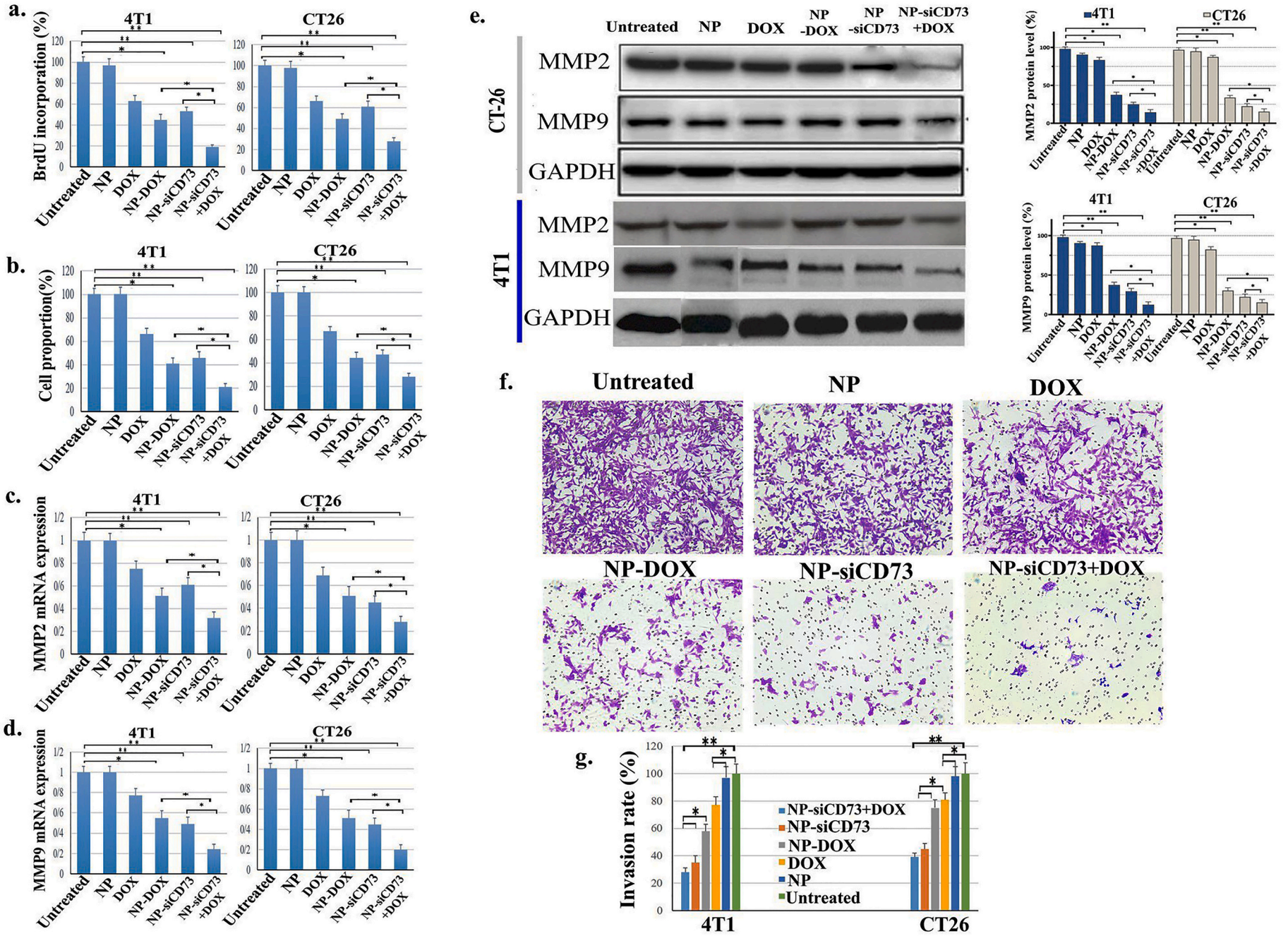

Fig. 4. Codelivery of siCD73 and DOX markedly inhibits proliferation and metastasis potential of cancer cells. Anti-proliferative impact of NPs loaded with siCD73 and DOX on 4T1 and CT26 cells was investigated by using BrdU (a) and Boyden chamber (b) assays. Anti-metastatic impact of combination therapy was also investigated by analyzing the expression of MMP9 and MMP2 genes (c–e) and invasion assay (f and g). (BrdU: Bromodeoxyuridine/5-bromo-2′-deoxyuridine).

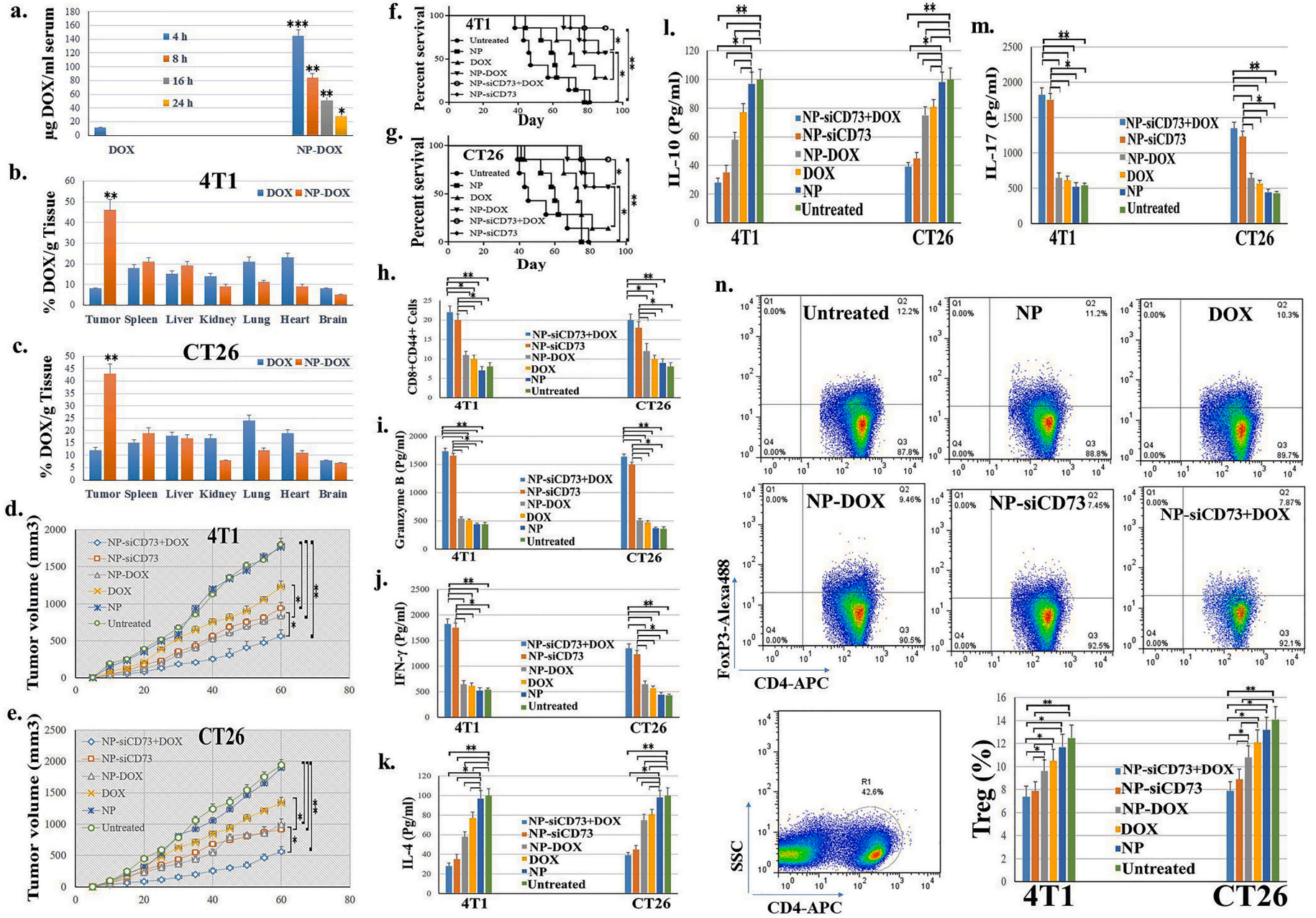

Fig. 5. Localization of NPs in the tumor site and simultaneous delivery of CD73 siRNA and DOX significantly suppress tumor growth and enhance anti-tumor immune responses. Biodistribution and DOX concentration in serum (a), tumor, and vital organs following intravenous administration of CL-TAT-H NPs loaded with DOX and free DOX in 4T1 (b) and CT26 (c) tumor-bearing mice at 24 h. Graphs show the effect of combination therapy on tumor volume (d and e) and survival rate (f and g) in two different tumor models. Codelivery of DOX and CD73 siRNA significantly enhanced the accumulation of effector $CD8^+$ T cells in tumor site (h). Moreover, combination therapy enhanced the granzyme B, IFN-γ, and IL-17, while reduced IL-4 and IL-10 secretion in the culture of tumor infiltrating leukocytes stimulated with tumor lysate [46]. Immunosuppressive Tregs were also downregulated in tumor bearing mice following treatment with NPs loaded with CD73 siRNA and DOX (n).

of CD73 siRNA loaded CL-TAT-HA NPs and DOX dramatically reduced cancer cell survival up to 48 h.

Flow cytometry assay was also performed to evaluate treatment groups' apoptotic effects on cancer cells using the annexin V-FITC/PI staining. As shown in Fig. 3f–g, therapeutic groups of NPs loaded with DOX and NP-CD73 siRNA could increase apoptosis in both cancer cell lines. Also, combination therapy group significantly increases the rate of apoptosis in these cell lines. What was evident in both MTT and flow cytometry analysis was that delivery of DOX using NPs increased the effect of the drug on cancer cell death. Its combination with CD73 silencing also increased the susceptibility of cancer cells to DOX-mediated death with an additive effect.

In order to investigate the mechanism of induced apoptosis by combination therapy, the expression of factors involved in cell survival including Bcl-2 and BIM was evaluated by qPCR and Western blotting. The data indicated that combination therapy additively increased BIM expression and decreased Bcl-2 expression in both cancer cell lines (Fig. 3h–j).

3.4. Codelivery of siCD73 and DOX markedly inhibits proliferation and metastasis potential of cancer cells

The BrdU assay was applied to investigate the suppressive impact of siRNA/DOX-loaded CL-TAT-HA NPs on cancer cell proliferation. As shown in Fig. 4a, the results showed that although both treatment groups of NPs loaded with CD73 siRNA or DOX alone could effectively inhibit cancer cell proliferation, the highest suppression of cancer cell proliferation capacity was observed in combination therapy group.

In addition, boyden chamber test was applied to examine the effect of therapy groups on cancer cell migration. The results showed that while both NP-DOX and NP-siRNA CD73 therapies could reduce cancer cell migration, the combination therapy group had the most significant migration reduction (Fig. 4b).

As important factors involved in the process of cancer cell metastasis, the expression of MMP2 and MMP9 factors was also evaluated at both mRNA and protein levels by qPCR and western blot tests. The data showed that combination therapy dramatically decreased MMP-2 and MMP-9 expression levels (Fig. 4c–e).

In addition, invasion assay performed to assess suppressive effect of siRNA/DOX-loaded CL-TAT-HA NPs in the invasion of cancer cells. As shown in Fig. 4f–g, the data showed that NP-DOX and NP-siRNA CD73 could somewhat decrease cancer cells' invasion. However, the highest rate of cancer cell invasion inhibition was observed in combination therapy by CD73 siRNA and DOX loaded NPs.

3.5. Accumulation of NPs in the tumor site and simultaneous delivery of CD73 siRNA and DOX significantly suppresses tumor growth and enhances anti-tumor immune responses

Biodistribution of NPs was performed using the DOX loaded in CL-TAT-HA NPs fluorescence signals. As shown Fig. 5a, the results showed that DOX loaded in NP was detectable in serum for a long time than free DOX. We also assessed the amount of DOX in the organs and tumor tissue of tumor-bearing mice 24 h after injection. As shown in Fig. 5b–c, there was no high concentration of free DOX at the tumor site after injection, while a high amount of DOX loaded on NPs was accumulated at the tumor site. The data also reported that small concentrations of DOX detected in the brain, kidneys, lungs.

Also, we investigated the effect of treatment groups on tumor growth in two different mouse xenograft models. As shown in Fig. 5d–e, although the CD73 siRNA-NP and NPs-DOX treated groups alone could significantly inhibit tumor growth, combination therapy by CD73-siRNA and DOX loaded CL-TAT-HA NPs had the maximum effect on reducing tumor growth.

Also, the survival rate of mice treated with different treatment groups was examined. As shown in Fig. 5f–g, combination therapy significantly enhanced survival rate compared to the control and single treatment groups.

In the next step, we investigated the effect of treatment groups on the immune responses in tumor-bearing mice. As shown in Fig. 5h, combination therapy by of CD73 siRNA and DOX loaded NPs compared to the control group can effectively increase $CD8^{+}CD44^{+}$ T cells in tumor samples, thereby enhancing antitumor responses. It should be noted that cells treated with NP-siCD73 could also increase the frequency of $CD8^{+}CD44^{+}$ T cells similar to what observed in combination therapy, while none of the other treatment groups had a significant effect on the frequency of these cells.

Also, to assess the impact of the treatment on the granzyme B, IFN-γ, IL-4, IL-10, and IL-17 secretion from T cells, these cells were collected from tumor tissue, stimulated with tumor lysate and secretion of these factors was evaluated by ELISA. The data showed that the highest increase in granzyme B, IFN-γ, and IL-17 secretion and the greatest decrease in IL-4 and IL-10 levels were observed after combination therapy and to lower extent by NP-siCD73 treatment. Similarly, none of the other therapeutic groups had a significant effect on the secretion of granzyme B, IFN-γ, IL-4, IL-10, and IL-17 (Fig. 5i–m).

Besides, the impact of treatment groups on the population of immune-suppressing Tregs was evaluated using Flow cytometry in tumor-bearing mice. The data showed that the combination therapy group and NP-siCD73 group could significantly inhibit the expansion of Treg cells in the tumor microenvironment; however, other therapeutic groups had no significant impact on the frequency of these cells (Fig. 5n).

3.6. Combination therapy by CD73 siRNA and DOX loaded NPs suppressed tumor necrosis and angiogenesis in tumor-bearing mice

To investigate the anti-angiogenic impact of combination therapy on angiogenesis in tumor-bearing mice, tumor histomorphometric characterization and vessel density was evaluated histologically by using the H&E staining of the tumor sections. As demonstrated in representative fields, the impact of combination therapy on tumor angiogenesis is significantly visible (Fig. 6a). Combination therapy and to a lesser extent CD73 siRNA and DOX loaded NPs notably reduced the number of blood vessels in tumor sections (Fig. 6b). Moreover, the hemoglobin levels in the tumor site, which indicate angiogenesis extent, reduced flowing treatment by CD73 siRNA and DOX loaded NPs (Fig. 6c).

As shown in Fig. 6d and e, histological analysis of paraffin-embedded tumor sections derived from control and treated mice indicated that the percentage of necrotic area was markedly decreased in tumors of CD73 siRNA and DOX loaded NPs.

4. Discussion

Cancer cells in the tumor microenvironment cause the spread and progression of carcinogenesis in the body by producing various secretory proteins, factors, and cytokines [43]. Adenosine is one of the most important secretory molecules in the tumor microenvironment that has a high ability to suppress immune responses. Adenosine concentration in the tumor site is approximately 20–30% higher than the normal site, which increases tumorigenesis [35,44]. Adenosine, produced from molecules such as CD39 and CD73 expressed on tumor and immune cells, can suppress immune responses by binding to adenosine receptors (AR) on Treg and MDSC cells [45,46]. Various studies have shown that suppression of immune responses can be prevented by inhibiting adenosine production [11,47–49]. One of these methods is to reduce the expression or block the CD73 molecule. The CD73 molecule has been reported to be overexpressed in different cancers and plays a crucial role in metastasis, angiogenesis, and tumor growth and blocking and inhibiting the CD73 molecule reduce tumorigenesis [50]. Various researches have reported that suppression of the CD73 molecule by various methods, such as CD73 -specific enzyme inhibitor (APCP) [51] or anti-

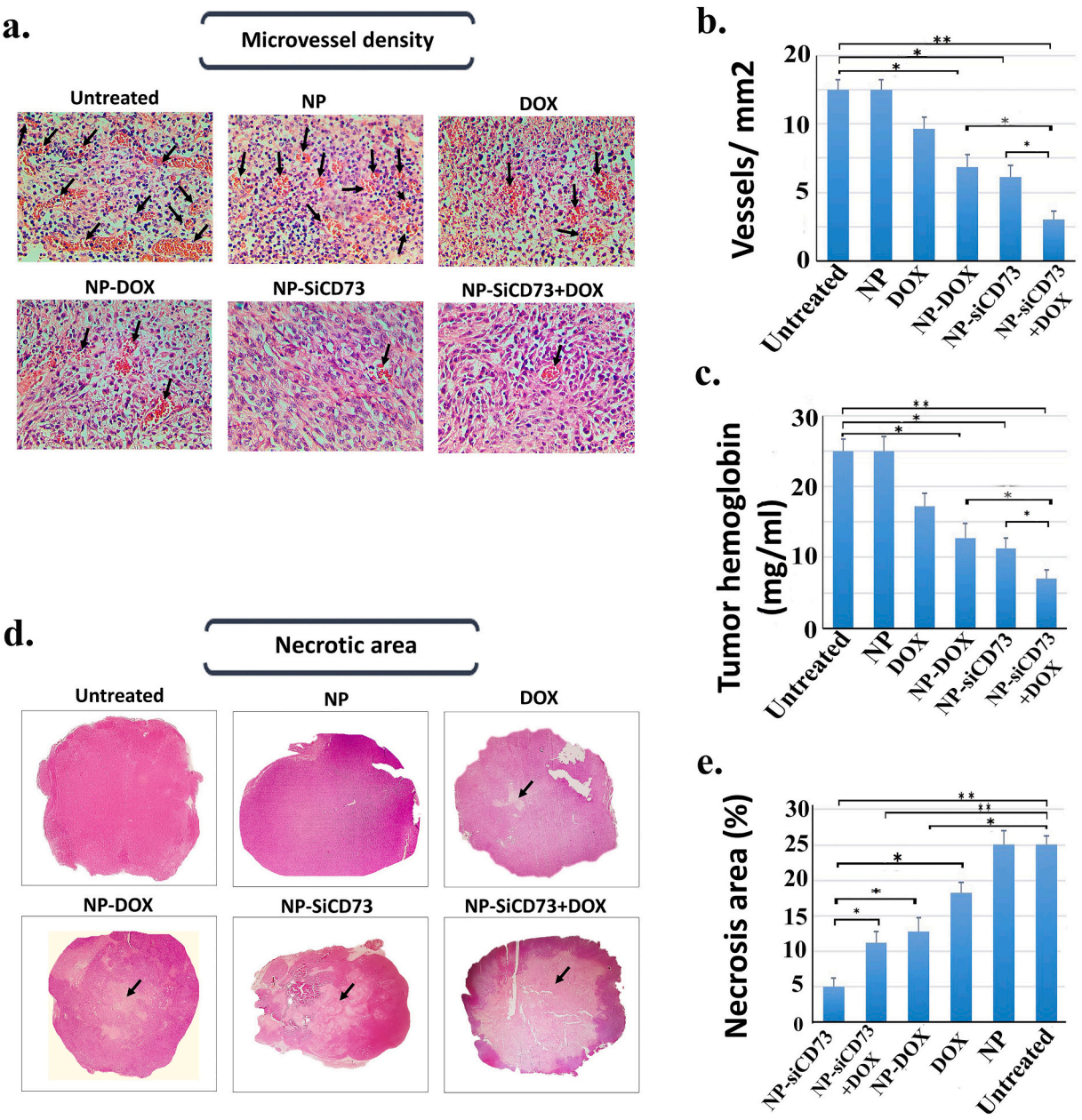

Fig. 6. Combination therapy by CD73 siRNA and DOX loaded NPs suppressed tumor necrosis and angiogenesis in tumor-bearing mice. Representative fields demonstrating the impact of combination therapy on of angiogenesis (A). The bar chart demonstrates the mean number of blood vessels evaluated in tumor sections (B). The bar chart shows the mean hemoglobin levels in tumor site as investigated by ELISA assay (C). Histopathological investigation by H&E staining with low and high magnifications, shows a central area of necrotic tissue in tumors (n = 4 per group) with treatment and non-treatment groups (d) and percentage of tumor necrotic area (e).

CD73 siRNA [40], can inhibit cancer development. The data from our previous studies indicate that the CD73 molecule can dramatically enhance metastasis and invasion of cancer cells [40,52]. Zhi et al. also reported that CD73 siRNA could inhibit the activity and expression of MMP-9 and MMP-2 and prevent breast cancer progression [53]. In another study, Azambuja reported that blocking CD73 could reduce the cell proliferation of glioma cancer cells [54].

On the other hand, CD73 expression has been shown to be associated with resistance to chemotherapy [55,56] and induce expression of CD73 in cancer cells [32,57]. Loi and colleagues have been shown that chemotherapy with DOX significantly increase CD73 expression in human breast cancer (MDA-231, MDA-468, SKBR3, BT474, ZR75, and T47D), melanoma (A2058 and LOX-1MV1), and leukemia (RPMI-8226 and Kasumi-1) cell lines. They demonstrated that systemic administration of DOX (2 mg/kg) in combination with anti-CD73 antibody or CD73 antagonists could significantly suppress tumor growth in tumor-bearing mice [32]. One of the major drawbacks of the previous report was the systemic administration of DOX, which can be associated with non-specific function with many cytotoxic and physiological side effects. Also, the performance of DOX following systemic administration requires the use of high doses. In addition, due to the expression of CD73 molecule as well as the very important physiological roles of CD73 and its product, adenosine, in different parts of the body, systemic inhibition of this molecule using monoclonal antibodies or antagonists can be associated with risk in the clinic. Based on these concerns, we decided to use a novel strategy to specifically inhibit CD73 in the tumor area and deliver DOX to cancer cells. Therefore, we designed and produced CL NPs functionalized with HIV-1 derived TAT peptide and HA polymer for

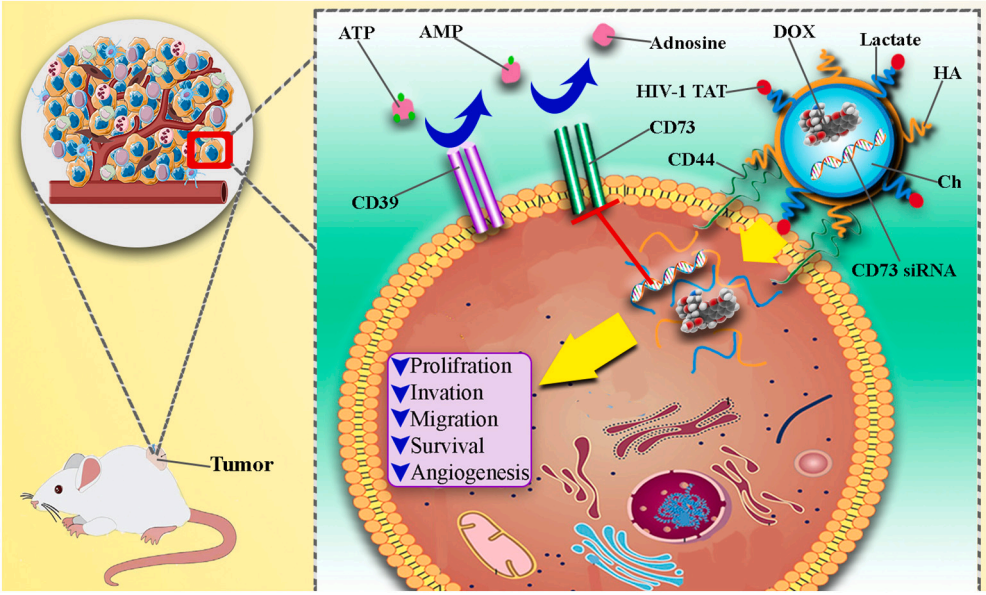

Fig. 7. Blockade of CD73 using siRNA loaded CL NPs functionalized with TAT-HA and loaded with DOX can effectively prevent tumor growth. CL-TAT-HA NPs could deliver DOX and anti-CD73 siRNA to cancer cells and significantly suppress the survival, invasion, proliferation, and migration of cancer cells.

simultaneous delivery of anti-CD73 siRNA and DOX to cancer cells. Firstly, the use of NPs means that we do need the minimum dose of DOX, and secondly, we have increased the efficiency of the minimum dose of DOX by inhibiting CD73. On the other hand, by inhibiting CD73, we solved the immunosuppression problem and thus increased the immune system responses. It has been shown that CL NPs are suitable for genes and drug delivery in treating gastrointestinal diseases, eye infections, and cancer therapy [58,59]. Our previous studies also showed that CL NPs have a very high ability for genes and drugs delivery, both *in vitro* and *in vivo* [31,60]. In this study, we applied HIV-1 TAT peptide to increase the cellular transfection ability of CL NPs. Accordingly, Rahmat and colleagues reported that coating of TAT peptide on chitosan-TGA/pDNA NPs increased the transfection efficiency and endosomal escape of these NPs [61]. Various studies have shown that HIV-1 TAT peptide has a high ability to bind to the neuropilin-1 receptor expressed in cancer cell lines such as CT26, 4T1, and MDA-MB-231, thereby increasing the cellular uptake of NPs conjugated to these peptides [62]. The HIV-1 TAT peptide can bind to the surface of the CL NPs *via* a disulfide bond. Studies have shown that disulfide (s-s) bonds can promote the stability of nanocarriers in the body's biological fluid and enhance the controlled release of NPs and the efficacy of gene therapy [63,64]. In addition to TAT peptide, we also conjugated the generated NPs with HA to facilitate CD44-mediated uptake of cancer cells. Accordingly, several studies have been shown that conjugating NPs with HA polymer, the main CD44 ligand expressed on various cancer cells, can be a useful technique for increasing the transfection of NPs into cancer cells through active targeting [33,65]. Zhang and colleagues also reported that HA-coated chitosan NPs (100–200 nm) efficiently deliver Cy3-labeled siRNA by binding to the CD44 receptor expressed in A549 cancer cells and prevent cancer progression by suppressing the Bcl2 gene [66]. One of our goals in this study was to reduce the effective dose of DOX by using targeted NPs and confine its effect to the tumor microenvironment. Our results showed that DOX transfer using CL-TAT-HA NPs could reduce the effective dose of this drug by about 2.5 times (Fig. 3a–c). Interestingly, our results showed that concomitant inhibition of the CD73 molecule could increase the susceptibility of cancer cells to DOX-induced death. Similarly, Qiao and coworkers showed that treatment of MDA-MB-231 and MDA-MB-468 cells with anti-CD73 antibody (3F7) could enhance cytotoxic effects of DOX in these cells [67]. After investigating the anti-cancer properties of targeted anti-CD73 siRNA and DOX delivery *in vitro*, the effect of this treatment strategy on tumor growth in two different mouse cancer models, the survival rate of mice, and the induction of anti-tumor immune responses were investigated. The results showed that combination therapy could effectively reduce tumor growth in both mouse models compared to other treatment groups. NP-siCD73 or NP-DOX could also significantly suppress tumor growth compared o control groups. Compared to the results obtained in the study of Loi et al., it can be concluded that the therapeutic strategy used in our study is more capable of controlling tumor growth. In their study, anti-CD73 antibody could not affect tumor growth. Moreover, they could not show a synergism impact of combinaded anti-CD73 antibody and DOX therapy. This difference in the effectiveness of the treatment strategy becomes more pronounced when we compare the survival results of mice; where in our study only one mouse died up to 90 days after combination therapy, whereas in the previous study all mice died within 65 days [32].

Regarding the effect of combination therapy on immune responses, our study showed that combination therapy and NP-siCD73 could increase the proliferation of effective $CD8^+$ T cells and increase the secretion of granzyme B and IFN-γ, IL-17, while reducing the abundance of IL-10 and IL-4 in the tumor site. On the other hand, NP-DOX and free DOX had little effect on either of these immune responses. In a study by Loi et al., a combination therapy of APCP (CD73 inhibitor) and DOX synergistically increased the frequency of antigen-specific $CD8^+$ T cells and secreted IFN-γ secretion. Surprisingly, they could not demonstrate induction of these immune responses following treatment of tumor-bearing mice with APCP alone [32], which was in contrast with our results. What may seem a bit contradictory at first glance in our study is why, given that DOX induces CD73 expression (Fig. 2c), little effect has been shown in suppressing immune responses in the tumor site. The answer is that although DOX can increase the expression of CD73 in tumor cells, due to its effect on reducing tumor size (by killing tumor cells) (Fig. 5d and e) it can decrease the number of cancer cells and reduce the pressure on the immune system in the tumor region. Based on our recent experience [37], we assumed our therapeutic approach may affect the induction of this critical tumor-promoting factor. So, we investigated the extent of vessel density and necrotic tumor area in various mice groups. Our results showed that downregulation of CD73 and administered DOX in tumors significantly reduced the vessel density and necrotic tumor area (Fig. 6).

These findings indicate that CL-TAT-HA NPs are a good candidate for co-delivery CD73 siRNA and DOX to cancer cells (Fig. 7), which should be further considered regarding safety and efficacy issues in various cancer patients.

CRediT authorship contribution statement

Armin Mahmoud Salehi Khesht: Conceptualization, Methodology, Writing - Original Draft, Software, Visualization.

Vahid Karpisheh: Writing - Review & Editing, Methodology.

Parisa Sahami Gilan: Writing - Review & Editing.

Lyubov A. Melnikova: Methodology, Software.

Angelina Olegovna Zekiy: Methodology, Writing - Review & Editing.

Mahdis Mohammadi: Investigation.

Mohammad Hojjat-Farsangi: Writing - Review & Editing.

Naime Majidi Zolbanin: Software.

Ata Mahmoodpoor: Methodology, Software.

Hadi Hassannia: Methodology.

Leili Aghebati-Maleki: Investigation.

Reza Jafari: Writing - Review & Editing.

Farhad Jadidi-Niaragh: Project administration, Conceptualization, Methodology, Writing -Review & Editing.

Declaration of competing interest

There is no conflict of interest.

Acknowledgment

This study was supported in part by grants provided by Urmia University of Medical Sciences (grant number: 2692), Tabriz University of Medical Sciences (grant numbers: 64010 and 65013), and National Institute for Medical Research Development, NIMAD, (grant number: 989658). We would also like to thank Taha Khezerloo and Mehrdad Khalili for their excellent contribution in this study.

References

[1] R. Baghban, L. Roshangar, R. Jahanban-Esfahlan, K. Seidi, A. Ebrahimi-Kalan, M. Jaymand, S. Kolahian, T. Javaheri, P. Zare, Tumor microenvironment complexity and therapeutic implications at a glance, Cell Commun. Signal. 18 (2020) 1–19.

[2] T.L. Whiteside, The tumor microenvironment and its role in promoting tumor growth, Oncogene 27 (2008) 5904–5912.

[3] P.I.R. Franco, A.P. Rodrigues, L.B. de Menezes, M.P. Miguel, Tumor microenvironment components: allies of cancer progression, Pathol. Res. Pract. 216 (2020), 152729.

[4] K. Kessenbrock, V. Plaks, Z. Werb, Matrix metalloproteinases: regulators of the tumor microenvironment, Cell 141 (2010) 52–67.

[5] H. Hassannia, M. Ghasemi Chaleshtari, F. Atyabi, M. Nosouhian, A. Masjedi, M. Hojjat-Farsangi, A. Namdar, G. Azizi, H. Mohammadi, G. Ghalamfarsa, Blockage of immune checkpoint molecules increases T-cell priming potential of dendritic cell vaccine, Immunology 159 (2020) 75–87.

[6] S. Izadi, A. Moslehi, H. Kheiry, F.K. Kiani, A. Ahmadi, A. Masjedi, S. Ghani, B. Rafiee, V. Karpisheh, F. Hajizadeh, Codelivery of HIF-1a siRNA and dinaciclib by carboxylated graphene oxide-trimethyl chitosan-hyaluronate nanoparticles significantly suppresses cancer cell progression, Pharm. Res. 37 (2020) 1–20.

[7] F. Jadidi-Niaragh, F. Atyabi, A. Rastegari, N. Kheshtchin, S. Arab, H. Hassannia, M. Ajami, Z. Mirsanei, S. Habibi, F. Masoumi, CD73 specific siRNA loaded chitosan lactate nanoparticles potentiate the antitumor effect of a dendritic cell vaccine in 4T1 breast cancer bearing mice, J. Control. Release 246 (2017) 46–59.

[8] V. Karpisheh, J.F. Afjadi, M.N. Afjadi, M.S. Haeri, T.S.A. Sough, S.H. Asl, M. Edalati, F. Atyabi, A. Masjedi, F. Hajizadeh, Inhibition of HIF-1a/EP4 axis by hyaluronate-trimethyl chitosan-SPION nanoparticles markedly suppresses the growth and development of cancer cells, Int. J. Biol. Macromol. 167 (2021 Jan 15) 1006–1019, https://doi.org/10.1016/j.ijbiomac.2020.11.056.

[9] Z.-W. Gao, K. Dong, H.-Z. Zhang, The roles of CD73 in cancer, Biomed. Res. Int. 2014 (2014).

[10] B. Zhang, CD73: a novel target for cancer immunotherapy, Cancer Res. 70 (2010) 6407–6411.

[11] F. Hajizadeh, S.M. Ardebili, M.B. Moornani, A. Masjedi, F. Atyabi, M. Kiani, A. Namdar, V. Karpisheh, S. Izadi, B. Baradaran, Silencing of HIF-1a/CD73 axis by siRNA-loaded TAT-chitosan-spion nanoparticles robustly blocks cancer cell progression, Eur. J. Pharmacol. 882 (2020), 173235.

[12] H. Dana, G.M. Chalbatani, H. Mahmoodzadeh, R. Karimloo, O. Rezaiean, A. Moradzadeh, N. Mehmandoost, F. Moazzen, A. Mazraeh, V. Marmari, Molecular mechanisms and biological functions of siRNA, Int. J. Biomed. Sci. 13 (2017) 48.

[13] Y. Li, T. Thambi, D.S. Lee, Co-delivery of drugs and genes using polymeric nanoparticles for synergistic cancer therapeutic effects, Adv. Healthc. Mater. 7 (2018) 1700886.

[14] M. Hosseini, M. Haji-Fatahaliha, F. Jadidi-Niaragh, J. Majidi, M. Yousefi, The use of nanoparticles as a promising therapeutic approach in cancer immunotherapy, Artif. Cells Nanomed. Biotechnol. 44 (2016) 1051–1061.

[15] F. Jadidi-Niaragh, M. Jeddi-Tehrani, B. Ansaripour, S.M. Razavi, R.A. Sharifian, F. Shokri, Reduced frequency of NKT-like cells in patients with progressive chronic lymphocytic leukemia, Med. Oncol. 29 (2012) 3561–3569.

[16] T. Ding, F. Yan, S. Cao, X. Ren, Regulatory B cell: new member of immunosuppressive cell club, Hum. Immunol. 76 (2015) 615–621.

[17] E. Mollarazi, A.R. Jalilian, F. Johari-daha, F. Atyabi, Development of 153Sm-folate-polyethyleneimine-conjugated chitosan nanoparticles for targeted therapy, J. Label. Compd. Radiopharm. 58 (2015) 327–335.

[18] W. Weecharangsan, P. Opanasopit, T. Ngawhirunpat, T. Rojanarata, A. Apirakaramwong, Chitosan lactate as a nonviral gene delivery vector in COS-1 cells, AAPS PharmSciTech 7 (2006) E74–E79.

[19] F. Talaei, E. Azizi, R. Dinarvand, F. Atyabi, Thiolated chitosan nanoparticles as a delivery system for antisense therapy: evaluation against EGFR in T47D breast cancer cells, Int. J. Nanomedicine 6 (2011) 1963.

[20] W. Weecharangsan, P. Opanasopit, T. Ngawhirunpat, A. Apirakaramwong, T. Rojanarata, U. Ruktanonchai, R.J. Lee, Evaluation of chitosan salts as non-viral gene vectors in CHO-K1 cells, Int. J. Pharm. 348 (2008) 161–168.

[21] S.W. Jones, R. Christison, K. Bundell, C.J. Voyce, S.M.V. Brockbank, P. Newham, M.A. Lindsay, Characterisation of cell-penetrating peptide-mediated peptide delivery, Br. J. Pharmacol. 145 (2005) 1093.

[22] F. Madani, S. Lindberg, Ü.F.S. Langel, A. Gräslund, Mechanisms of cellular uptake of cell-penetrating peptides, J. Biophys. (2011) 1–10, in.

[23] A. Almalik, H. Benabdelkamel, A. Masood, I.O. Alanazi, I. Alradwan, M. A. Majrashi, A.A. Alfadda, W.M. Alghamdi, H. Alrabiah, N. Tirelli, Hyaluronic acid coated chitosan nanoparticles reduced the immunogenicity of the formed protein corona, Sci. Rep. 7 (2017) 1–9.

[24] E. Vismara, C. Bongio, A. Coletti, R. Edelman, A. Serafini, M. Mauri, R. Simonutti, S. Bertini, E. Urso, Y.G. Assaraf, Albumin and hyaluronic acid-coated superparamagnetic iron oxide nanoparticles loaded with paclitaxel for biomedical applications, Molecules 22 (2017) 1030.

[25] G.H. Wang, Y.Y. Cai, J.K. Du, L. Li, Q. Li, H.K. Yang, J.T. Lin, TAT-conjugated chitosan cationic micelle for nuclear-targeted drug and gene co-delivery, Colloids Surf. B: Biointerfaces 162 (2018) 326–334.

[26] H.-H. Peng, D.-X. Hong, Y.-X. Guan, S.-J. Yao, Preparation of pH-responsive DOX-loaded chitosan nanoparticles using supercritical assisted atomization with an enhanced mixer, Int. J. Pharm. 558 (2019) 82–90.

[27] A. Masjedi, H. Hassannia, F. Atyabi, A. Rastegari, M. Hojjat-Farsangi, A. Namdar, H. Soleimanpour, G. Azizi, A. Nikkhoo, G. Ghalamfarsa, Downregulation of A2AR by siRNA loaded PEG-chitosan-lactate nanoparticles restores the T cell mediated anti-tumor responses through blockage of PKA/CREB signaling pathway, Int. J. Biol. Macromol. 133 (2019) 436–445.

[28] D.R. Bienek, K.M. Hoffman, W. Tutak, Blow-spun chitosan/PEG/PLGA nanofibers as a novel tissue engineering scaffold with antibacterial properties, J. Mater. Sci. Mater. Med. 27 (2016) 1–10.

[29] T.S.C. Li, T. Yawata, K. Honke, Efficient siRNA delivery and tumor accumulation mediated by ionically cross-linked folic acid–poly (ethylene glycol)–chitosan oligosaccharide lactate nanoparticles: for the potential targeted ovarian cancer gene therapy, Eur. J. Pharm. Sci. 52 (2014) 48–61.

[30] S. Bastaki, S. Aravindhan, N.A. Saheb, M.A. Kashani, A.E. Dorofeev, F.K. Kiani, H. Jahandideh, F.B. Dargani, M. Aksoun, A. Nikkhoo, Codelivery of STAT3 and PD-L1 siRNA by hyaluronate-TAT trimethyl/thiolated chitosan nanoparticles suppresses cancer progression in tumor-bearing mice, Life Sci. 266 (2021), 118847.

[31] S. Salimifard, F.K. Kiani, F.S. Eshaghi, S. Izadi, K. Shahdadnejad, A. Masjedi, M. Heydari, A. Ahmadi, M. Hojjat-Farsangi, H. Hassannia, Codelivery of BV6 and anti-IL6 siRNA by hyaluronate-conjugated PEG-chitosan-lactate nanoparticles inhibits tumor progression, Life Sci. 260 (2020), 118423.

[32] S. Loi, S. Pommey, B. Haibe-Kains, P.A. Beavis, P.K. Darcy, M.J. Smyth, J. Stagg, CD73 promotes anthracycline resistance and poor prognosis in triple negative breast cancer, Proc. Natl. Acad. Sci. 110 (2013) 11091–11096.

[33] S. Song, H. Qi, J. Xu, P. Guo, F. Chen, F. Li, X. Yang, N. Sheng, Y. Wu, W. Pan, Hyaluronan-based nanocarriers with CD44-overexpressed cancer cell targeting, Pharm. Res. 31 (2014) 2988–3005.

[34] V. Karpisheh, Inhibition of Cancer Cell Growth and Proliferation by Combination Therapy With Inhibition of Hypoxia-induced Factor (HIF-1a) and EP4 Receptor, 2020.

[35] F. Jadidi-Niaragh, F. Atyabi, A. Rastegari, E. Mollarazi, M. Kiani, A. Razavi, M. Yousefi, N. Kheshtchin, H. Hassannia, J. Hadjati, Downregulation of CD73 in 4T1 breast cancer cells through siRNA-loaded chitosan-lactate nanoparticles, Tumor Biol. 37 (2016) 8403–8412.

[36] N. Joshi, F. Hajizadeh, E.A. Dezfouli, A.O. Zekiy, M.N. Afjadi, S.M. Mousavi, M. Hojjat-Farsangi, V. Karpisheh, A. Mahmoodpoor, H. Hassannia, Silencing STAT3 enhances sensitivity of cancer cells to doxorubicin and inhibits tumor progression, Life Sci. 119369 (2021).

[37] N. Kheshtchin, S. Arab, M. Ajami, R. Mirzaei, M. Ashourpour, N. Mousavi, N. Khosravianfar, F. Jadidi-Niaragh, A. Namdar, F. Noorbakhsh, Inhibition of HIF-

1a enhances anti-tumor effects of dendritic cell-based vaccination in a mouse model of breast cancer, Cancer Immunol. Immunother. 65 (2016) 1159–1167.
[38] T. Yan, S. Zhu, W. Hui, J. He, Z. Liu, J. Cheng, Chitosan based pH-responsive polymeric prodrug vector for enhanced tumor targeted co-delivery of doxorubicin and siRNA, Carbohydr. Polym. 250 (2020), 116781.
[39] J. Shi, L. Wang, J. Zhang, R. Ma, J. Gao, Y. Liu, C. Zhang, Z. Zhang, A tumor-targeting near-infrared laser-triggered drug delivery system based on GO@ ag nanoparticles for chemo-photothermal therapy and X-ray imaging, Biomaterials 35 (2014) 5847–5861.
[40] S. Hallaj, S.H. Asl, F. Alian, S. Farshid, F.S. Eshaghi, A. Namdar, F. Atyabi, A. Masjedi, T. Hallaj, A. Ghorbani, Inhibition of CD73 using folate targeted nanoparticles carrying anti-CD73 siRNA potentiates anticancer efficacy of dinaciclib, Life Sci. 259 (2020), 118150.
[41] S. Bastaki, S. Aravindhan, N.A. Saheb, M.A. Kashani, A.E. Dorofeev, F.K. Kiani, H. Jahandideh, F.B. Dargani, M. Aksoun, A. Nikkhoo, Codelivery of STAT3 and PD-L1 siRNA by hyaluronate-TAT trimethyl/thiolated chitosan nanoparticles suppresses cancer progression in tumor-bearing mice, Life Sci. 118847 (2020).
[42] A. Masjedi, A. Ahmadi, S. Ghani, F. Malakotikhah, M.N. Afjadi, M. Irandoust, F. K. Kiani, S.H. Asl, F. Atyabi, H. Hassannia, Silencing adenosine A2a receptor enhances dendritic cell-based cancer immunotherapy, nanomedicine: nanotechnology, Biol. Med. 29 (2020), 102240.
[43] C. Roma-Rodrigues, R. Mendes, P.V. Baptista, A.R. Fernandes, Targeting tumor microenvironment for cancer therapy, Int. J. Mol. Sci. 20 (2019) 840.
[44] J. Blay, T.D. White, D.W. Hoskin, The extracellular fluid of solid carcinomas contains immunosuppressive concentrations of adenosine, Cancer Res. 57 (1997) 2602–2605.
[45] B.N. Cronstein, G. Haskó, Regulation of inflammation by adenosine, Front. Immunol. 4 (2013) 85.
[46] V. Karpisheh, S.M. Mousavi, P.N. Sheykholeslami, M. Fathi, M.M. Saray, L. Aghebati-Maleki, R. Jafari, N.M. Zolbanin, F. Jadidi-Niaragh, The role of regulatory T cells in the pathogenesis and treatment of prostate cancer, Life Sci. 119132 (2021).
[47] D.W. Hoskin, Adenosine as a possible inhibitor of killer T-cell activation in the microenvironment of solid tumors, Int. J. Cancer 59 (1994) 854–855.
[48] D.W. Hoskin, T. Reynolds, J. Blay, Colon adenocarcinoma cells inhibit anti-CD3-activated killer cell induction, Cancer Immunol. Immunother. 38 (1994) 201–207.
[49] W.M. MacKenzie, D.W. Hoskin, J. Blay, Adenosine suppresses a4ß7 integrin-mediated adhesion of T lymphocytes to colon adenocarcinoma cells, Exp. Cell Res. 276 (2002) 90–100.
[50] D. Jin, J. Fan, L. Wang, L.F. Thompson, A. Liu, B.J. Daniel, T. Shin, T.J. Curiel, B. Zhang, CD73 on tumor cells impairs antitumor T-cell responses: a novel mechanism of tumor-induced immune suppression, Cancer Res. 70 (2010) 2245–2255.
[51] C.M. Hay, E. Sult, Q. Huang, K. Mulgrew, S.R. Fuhrmann, K.A. McGlinchey, S. A. Hammond, R. Rothstein, J. Rios-Doria, E. Poon, Targeting CD73 in the tumor microenvironment with MEDI9447, Oncoimmunology 5 (2016), e1208875.
[52] K.O. Alzamely, F. Hajizadeh, M. Heydari, M.J.G. Sede, S.H. Asl, M. Peydaveisi, A. Masjedi, S. Izadi, A. Nikkhoo, F. Atyabi, Combined inhibition of CD73 and ZEB1 by arg-gly-asp (RGD)-targeted nanoparticles inhibits tumor growth, Colloids Surf. B: Biointerfaces 197 (2020), 111421.
[53] X. Zhi, S. Chen, P. Zhou, Z. Shao, L. Wang, Z. Ou, L. Yin, RNA interference of ecto-5'-nucleotidase (CD73) inhibits human breast cancer cell growth and invasion, Clin. Exp. Metastasis 24 (2007) 439–448.
[54] J.H. Azambuja, N.E. Gelsleichter, L.R. Beckenkamp, I.C. Iser, M.C. Fernandes, F. Figueiró, A.M.O. Battastini, J.N. Scholl, F.H. de Oliveira, R.M. Spanevello, CD73 downregulation decreases in vitro and in vivo glioblastoma growth, Mol. Neurobiol. 56 (2019) 3260–3279.
[55] P. Ujházy, M. Klobušická, O. Babušíková, P. Strausbauch, E. Mihich, M.J. Ehrke, Ecto-5'-nucleotidase (CD73) in multidrug-resistant cell lines generated by doxorubicin, Int. J. Cancer 59 (1994) 83–93.
[56] P. Ujházy, E.S. Berleth, J.M. Pietkiewicz, H. Kitano, J.R. Skaar, M.J. Ehrke, E. Mihich, Evidence for the involvement of ecto-5'-nucleotidase (CD73) in drug resistance, Int. J. Cancer 68 (1996) 493–500.
[57] D. Samanta, Y. Park, X. Ni, H. Li, C.A. Zahnow, E. Gabrielson, F. Pan, G.L. Semenza, Chemotherapy induces enrichment of CD47+/CD73+/PDL1+ immune evasive triple-negative breast cancer cells, Proc. Natl. Acad. Sci. 115 (2018) E1239–E1248.
[58] N.L. Ignjatovic, M. Sakac, I. Kuzminac, V. Kojic, S. Markovic, D. Vasiljevic-Radovic, V.M. Wu, V. Uskokovic, D.P. Uskokovic, Chitosan oligosaccharide lactate coated hydroxyapatite nanoparticles as a vehicle for the delivery of steroid drugs and the targeting of breast cancer cells, J. Mater. Chem. B 6 (2018) 6957–6968.
[59] M.A. Mohammed, J. Syeda, K.M. Wasan, E.K. Wasan, An overview of chitosan nanoparticles and its application in non-parenteral drug delivery, Pharmaceutics 9 (2017) 53.
[60] A. Masjedi, A. Ahmadi, S. Ghani, F. Malakotikhah, M. Nabi Afjadi, M. Irandoust, F. Karoon Kiani, S. Heydarzadeh Asl, F. Atyabi, H. Hassannia, M. Hojjat-Farsangi, A. Namdar, G. Ghalamfarsa, F. Jadidi-Niaragh, Silencing adenosine A2a receptor enhances dendritic cell-based cancer immunotherapy, Nanomedicine 29 (2020), 102240.
[61] D. Rahmat, M.I. Khan, G. Shahnaz, D. Sakloetsakun, G. Perera, A. Bernkop-Schnürch, Synergistic effects of conjugating cell penetrating peptides and thiomers on non-viral transfection efficiency, Biomaterials 33 (2012) 2321–2326.
[62] M.P. Barr, A.M. Byrne, A.M. Duffy, C.M. Condron, M. Devocelle, P. Harriott, D. J. Bouchier-Hayes, J.H. Harmey, A peptide corresponding to the neuropilin-1-binding site on VEGF 165 induces apoptosis of neuropilin-1-expressing breast tumour cells, Br. J. Cancer 92 (2005) 328–333.
[63] R.P. Ahwazi, M. Kiani, M. Dinarvand, A. Assali, F.S.M. Tekie, R. Dinarvand, F. Atyabi, Immobilization of HIV-1 TAT peptide on gold nanoparticles: a feasible approach for siRNA delivery, J. Cell. Physiol. 235 (2020) 2049–2059.
[64] K.S. Rao, M.K. Reddy, J.L. Horning, V. Labhasetwar, TAT-conjugated nanoparticles for the CNS delivery of anti-HIV drugs, Biomaterials 29 (2008) 4429–4438.
[65] B.B. Karakocak, J. Liang, P. Biswas, N. Ravi, Hyaluronate coating enhances the delivery and biocompatibility of gold nanoparticles, Carbohydr. Polym. 186 (2018) 243–251.
[66] W. Zhang, W. Xu, Y. Lan, X. He, K. Liu, Y. Liang, Antitumor effect of hyaluronic-acid-modified chitosan nanoparticles loaded with siRNA for targeted therapy for non-small cell lung cancer, Int. J. Nanomedicine 14 (2019) 5287.
[67] Z. Qiao, X. Li, N. Kang, Y. Yang, C. Chen, T. Wu, M. Zhao, Y. Liu, X. Ji, A novel specific anti-CD73 antibody inhibits triple-negative breast cancer cell motility by regulating autophagy, Int. J. Mol. Sci. 20 (2019) 1057.